Cell Reports, Volume *41*

Supplemental information

Consumption of fish oil high-fat diet induces murine hair loss via epidermal fatty acid binding protein in skin macrophages

Jiaqing Hao, Rong Jin, Jun Zeng, Yuan Hua, Matthew S. Yorek, Lianliang Liu, Anita Mandal, Junling Li, Huaiyu Zheng, Yanwen Sun, Yanmei Yi, Di Yin, Qi Zheng, Xiaohong Li, Chin K. Ng, Eric C. Rouchka, Nejat K. Egilmez, Ali Jabbari, and Bing Li

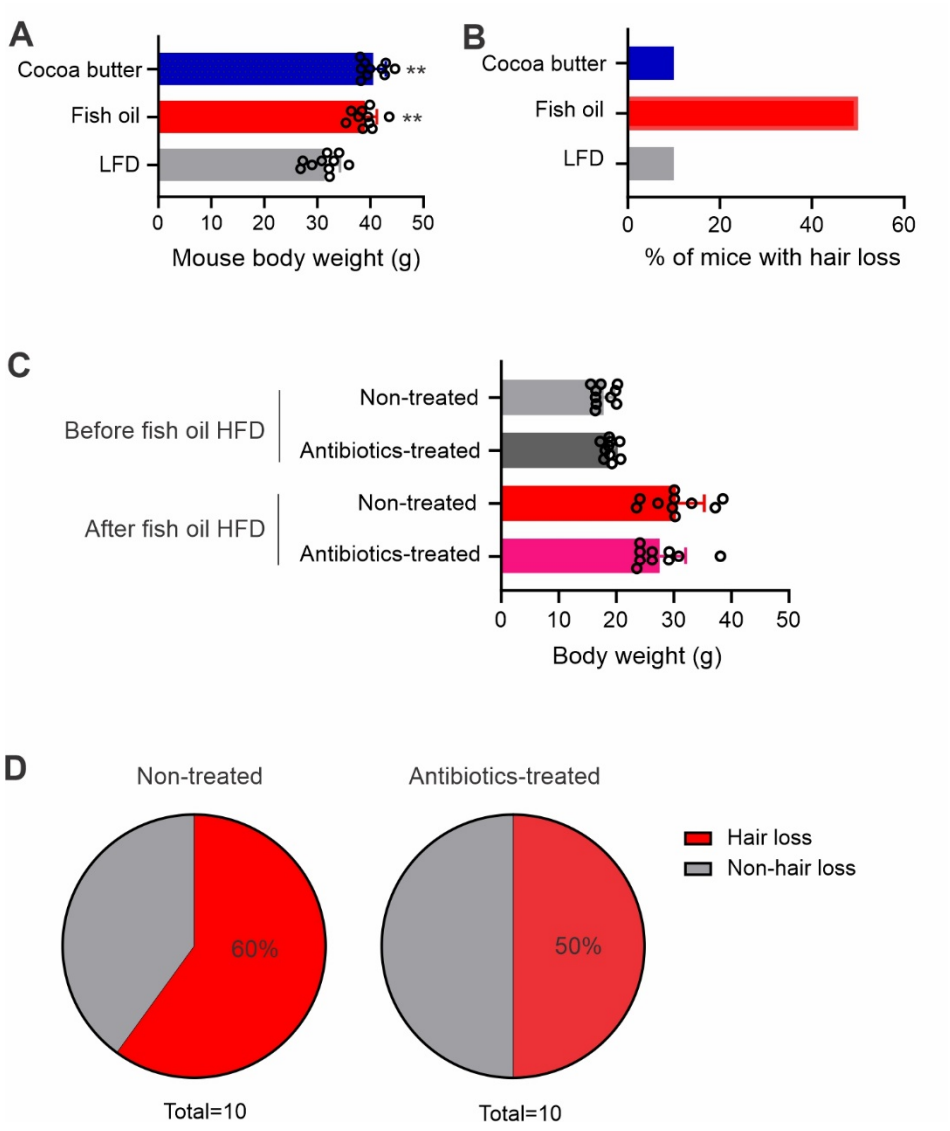

Figure S1. Fish oil HFD-induced murine hair loss is independent on gut microbiota. Related to Figure 1. (A) Body weight of male mice fed the LFD, cocoa butter HFD, or fish oil HFD for 3 months (n=10/group) (**p<0.01 as compared to LFD group, unpaired Student t test). (B) Average percentage of hair loss mice fed the indicated diets for 3 months (n=10/group). (C) Body weight of female mice (n=10/group) fed the fish oil HFD with or without antibiotics (200mg /L streptomycin and vancomycin in drinking water) for 3 months. (D) Percentage of fish oil HFD-induced hair loss mice with or without antibiotic treatment for 3 months.

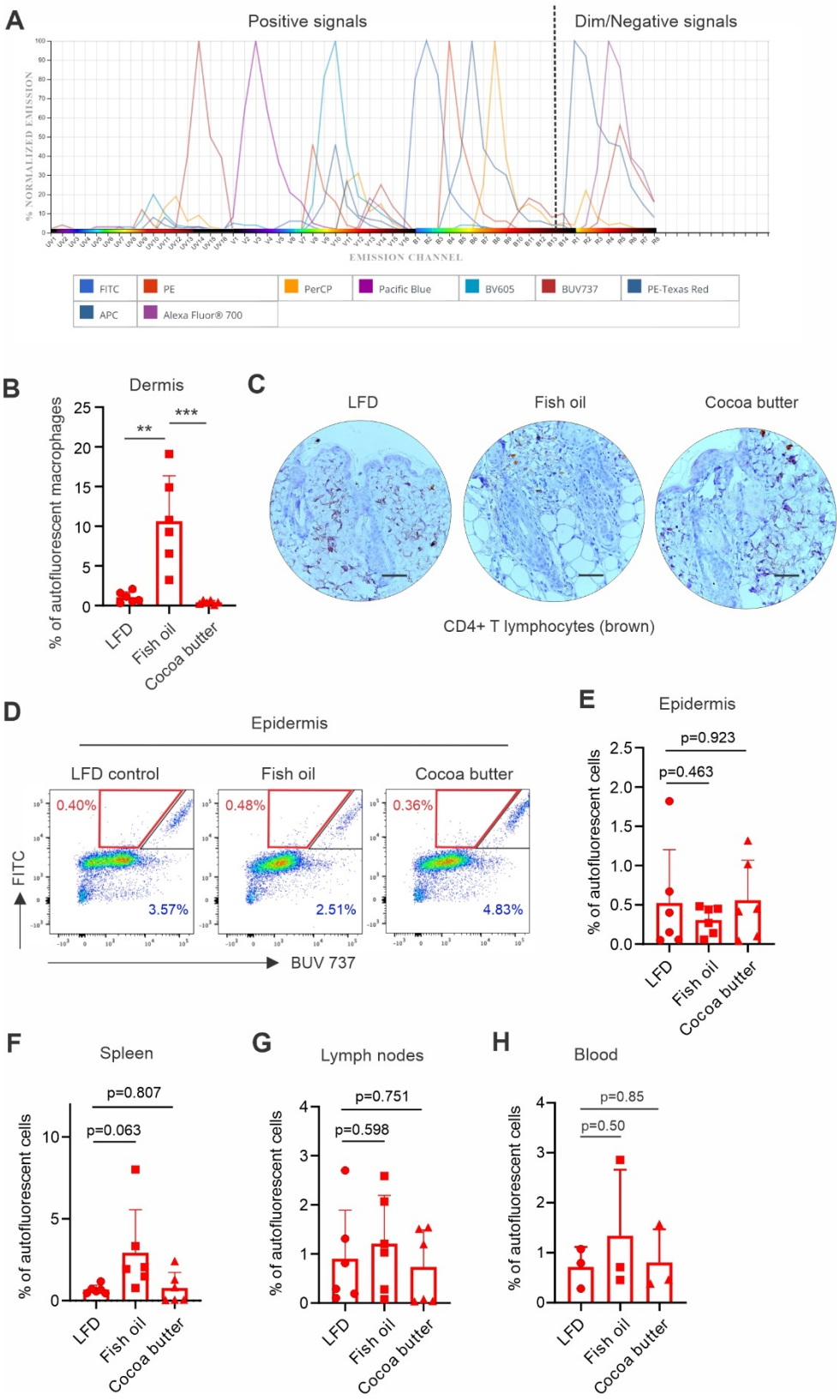
A
Positive signals
Dim/Negative signals
% NORMALIZED EMISSION
EMISSION CHANNEL
FITC
PE
PerCP
Pacific Blue
BV605
BUV737
PE-Texas Red
APC
Alexa Fluor® 700
B
Dermis
% of autofluorescent macrophages
**
***
LFD
Fish oil
Cocoa butter
C
LFD
Fish oil
Cocoa butter
CD4+ T lymphocytes (brown)
D
Epidermis
LFD control
Fish oil
Cocoa butter
0.40%
3.57%
0.48%
2.51%
0.36%
4.83%
FITC
BUV 737
E
Epidermis
% of autofluorescent cells
p=0.923
p=0.463
F
Spleen
p=0.807
p=0.063
G
Lymph nodes
p=0.751
p=0.598
H
Blood
p=0.85
p=0.50

Figure S2. Phenotypic analysis of auto-fluorescent macrophages in mice fed the LFD, fish oil HFD or cocoa butter HFD. Related to Figure 2. (A) Spectrum of fluorescent dyes used for immune cell phenotypic analysis by fluorescent-based flow cytometry. (B) Dermal cells were separated from mice fed the indicated diets. Average percentage of the auto-fluorescent macrophages in the dermis were analyzed by flow cytometric staining (n=6/group). (C) IHC analysis of $CD4^+$ T cells (brown) in the skin of mice fed the LFD, fish oil HFD or cocoa butter HFD for 3 months. Scale bar, 100μM. (D, E) Epidermal cells were separated from mice fed the indicated diets. The auto-fluorescent macrophages were analyzed with the same gating strategy as dermis by flow cytometric staining. Average percentage of the auto-fluorescent cells in skin epidermis is shown in panel E (n=6/group). (F-H) Flow cytometric analysis of auto-fluorescent macrophages in spleen (n=6/group) (F), lymph nodes (n=6/group) (G), and peripheral blood (n=3/group) (H) in mice fed the indicated diets for 3 months. Data are shown as mean ± SD (*** $p<0.001$, ** $p<0.01$, unpaired Student t test).

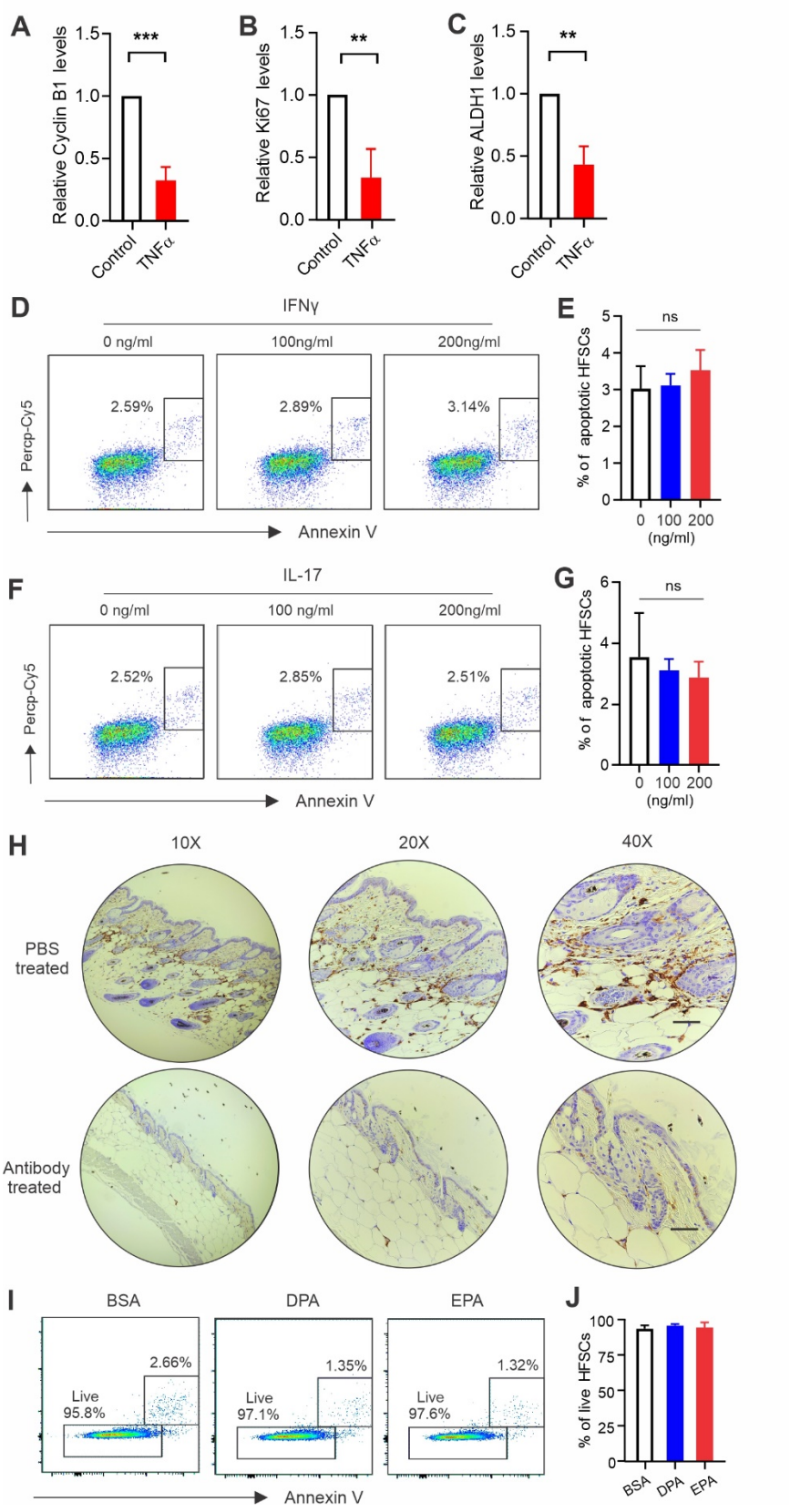
A
Relative Cyclin B1 levels
1.5
1.0
0.5
0.0
***
Control
TNFα
B
Relative Ki67 levels
**
C
Relative ALDH1 levels
D
IFNγ
0 ng/ml
100ng/ml
200ng/ml
Percp-Cy5
2.59%
2.89%
3.14%
Annexin V
E
ns
% of apoptotic HFSCs
0 100 200
(ng/ml)
F
IL-17
0 ng/ml
100 ng/ml
200ng/ml
2.52%
2.85%
2.51%
G
H
10X
20X
40X
PBS treated
Antibody treated
I
BSA
DPA
EPA
2.66%
1.35%
1.32%
Live 95.8%
Live 97.1%
Live 97.6%
J
% of live HFSCs
100
75
50
25
0
BSA
DPA
EPA

Figure S3. Apoptosis of HFSCs is independent of IFNγ, IL-17 and n-3 FA itself. Related to Figure 3. (A-C) Real-time PCR analysis of cyclin B1 (A), Ki67 (B), and ALDH1 (C) expression in mouse HFSCs treated with TNFα (100ng/ml) or medium control overnight (n=3/group). (D, E) Flow cytometric analysis of different pathological levels of IFNγ-mediated HFSC apoptosis using Annexin V staining. Average percentage of IFNγ-induced apoptotic HFSCs is shown in panel E(n=3/group). (F, G) Flow cytometric analysis of different pathological levels of IL-17-mediated HFSC apoptosis using Annexin V staining. Average percentage of IL-17-induced apoptotic HFSCs is shown in panel G(n=3/group). (H) Mice with fish oil HFD-induced hair loss were treated either with anti-TNF antibody or control PBS for 4 weeks. $F4/80^+$ macrophage accumulation was analyzed by IHC staining (brown, $F4/80^+$ cells). Scale bar, 100μM. (I, J) Flow cytometric analysis of the indicated n-3 FA-induced apoptosis of HFSCs using Annexin V staining. Average percentage of live HFSC treated with BSA, DPA or EPA (200μM) is shown in panel J (n=3/group). Data are shown as mean ± SD (*** $p<0.001$, ** $p<0.01$, ns: non-significance, unpaired Student t test).

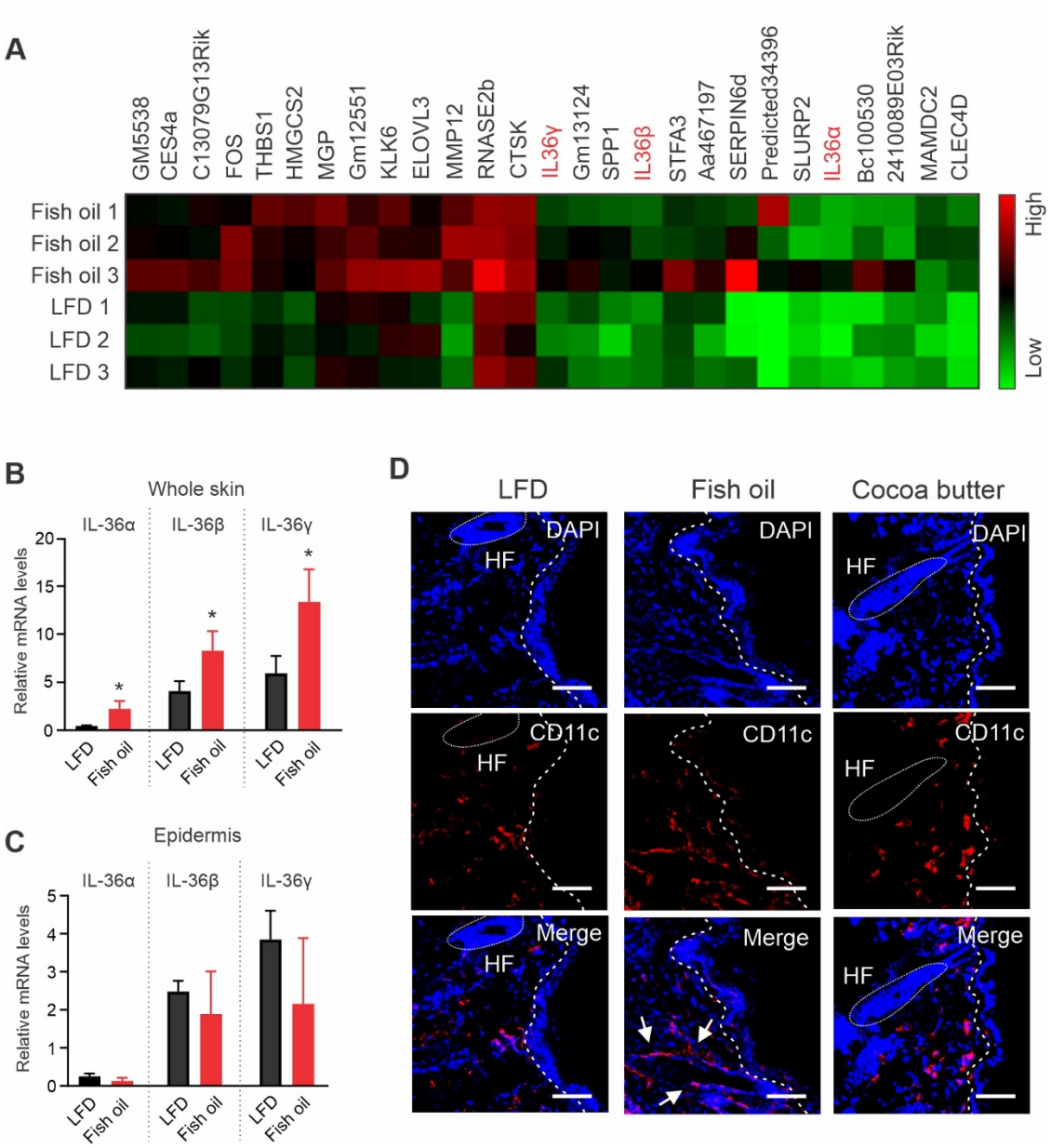

Figure S4. Fish oil HFD induces IL-36 signaling in skin dermis. Related to Figure 4. (A) Heatmap of differentially expressed genes specifically upregulated by the fish oil HFD. (B) Real-time PCR analysis of the expression of IL-36 family members in whole skin tissues from mice fed the LFD or fish oil HFD for 3 months (*, $p<0.05$ compared to the LFD diet, n=3/group, unpaired Student t test). (C) Real-time PCR analysis of IL-36 gene expression in skin epidermis from mice fed the LFD or fish oil HFD for 3 months (n=3/group). (D) Confocal microscopy staining of $CD11c^+$ macrophage distribution in the skin of mice fed the LFD, fish oil HFD or cocoa butter HFD (white arrows: $CD11c^+$ macrophages; HF: hair follicle). Scale bar: 50μM.

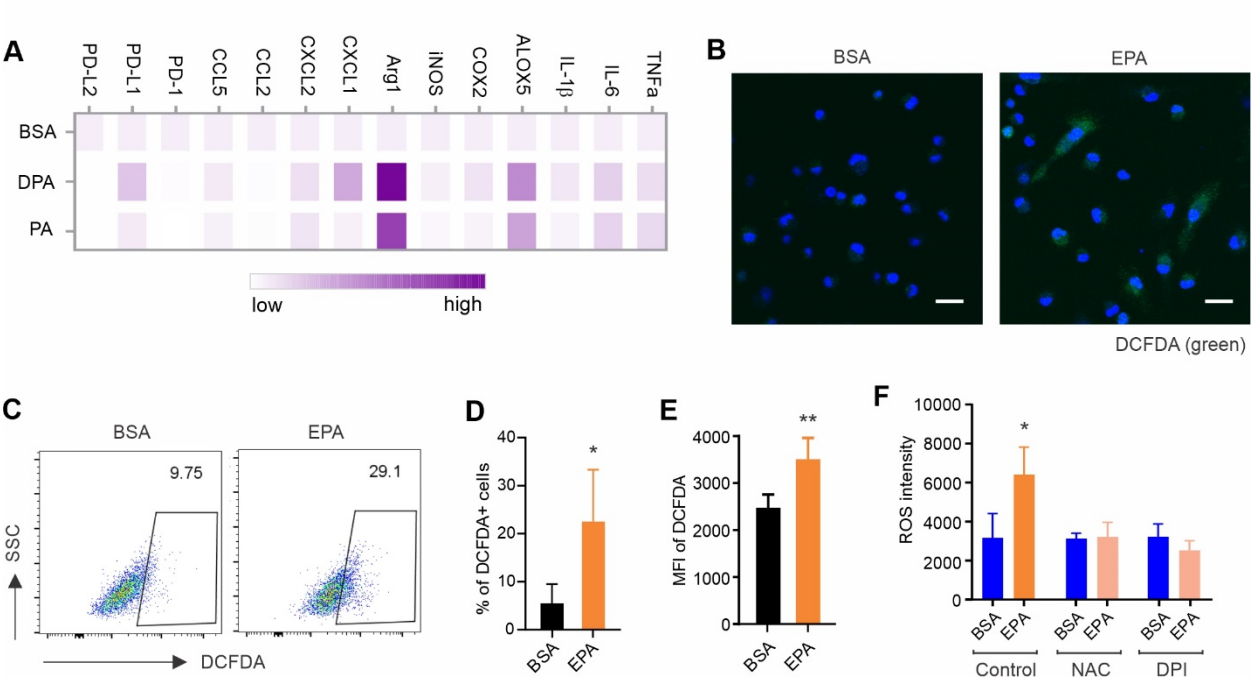

Figure S5. n-3 FA treatment induces ROS production in CD11c⁺ macrophages. Related to Figure 5. (A) Real-time PCR analysis of expression profile of FA-related cytokines, chemokines and enzymes in CD11c⁺ macrophages treated with 200μM DPA, PA or control BSA for 24h. (B) Analysis of 200μM EPA-induced ROS production in CD11c⁺ macrophages by confocal microscopy (green: DCFDA, blue: DAPI for nuclei). Scale bar, 20μM. (C-E) Flow cytometric analysis of EPA-induced ROS production in CD11c⁺ macrophages as shown by percentage (D) and mean fluorescent intensity (MFI) (E) of DCFDA (*p<0.05, **p<0.01 as compared to BSA control, n=3/group). (F) Flow cytometric analysis of EPA-induced ROS production in CD11c⁺ macrophages in the presence or absence of ROS inhibitors NAC or DPI (*p<0.05 as compared to BSA control, n=3/group, unpaired Student t test).

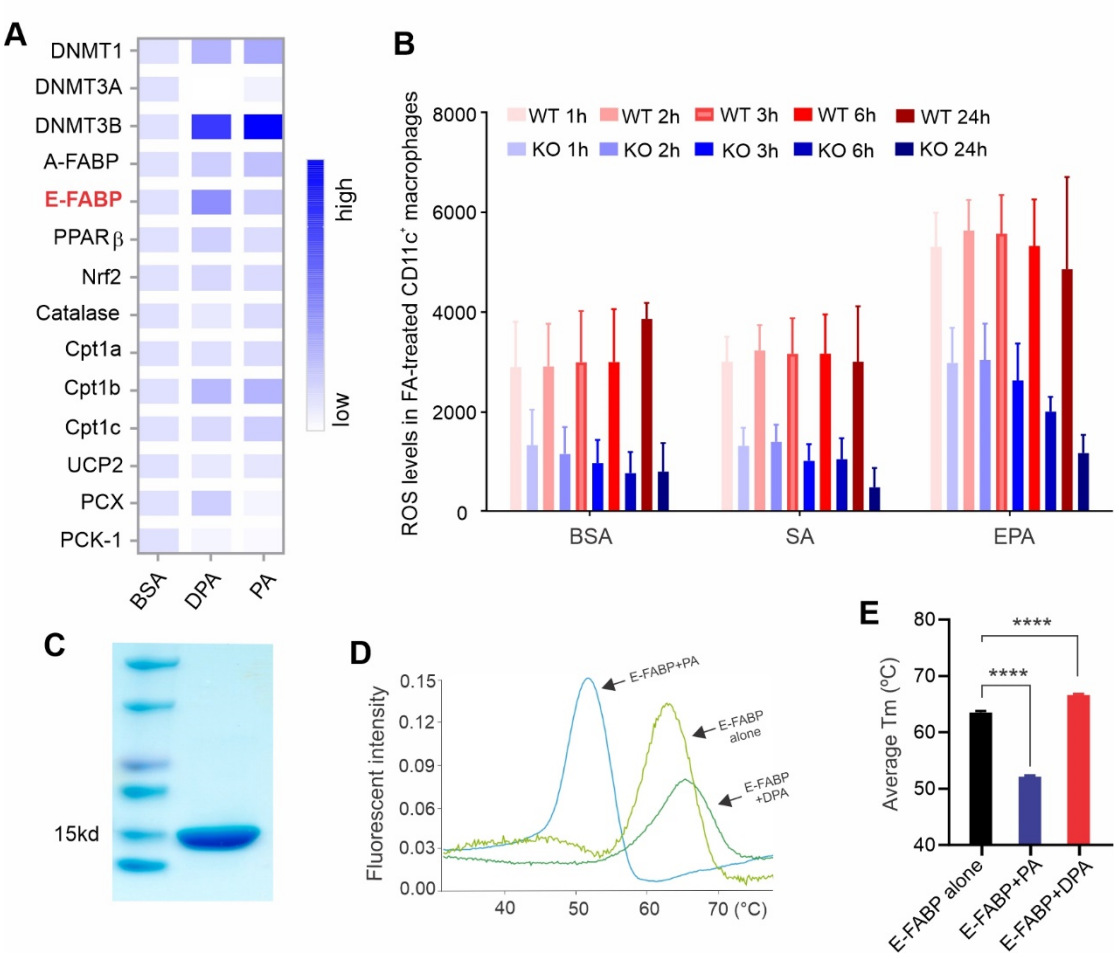

Figure S6. E-FABP mediates n-3 FA-induced ROS production in macrophages. Related to Figure 6. (A) Real-time PCR analysis of the expression profile of molecules associated with FA metabolism in $CD11c^{+}$ macrophages treated with 200μM DPA, PA or BSA for 24h. (B) ROS production in WT and E-$FABP^{-/-}$ $CD11c^{+}$ macrophages treated with 200μM SA, EPA or BSA (n=3/group), respectively, at the indicated time points. (C) SDS-page gel of mouse recombinant E-FABP purified from *E.coli.* (D, E) Thermal shift assay measuring the binding of PA, DPA to E-FABP. Average Tm value of E-FABP/FA binding assay is shown in panel E (n=3/group). Data are shown as mean ± SD (**** $p<0.0001$, *** $p<0.001$, unpaired Student t test).

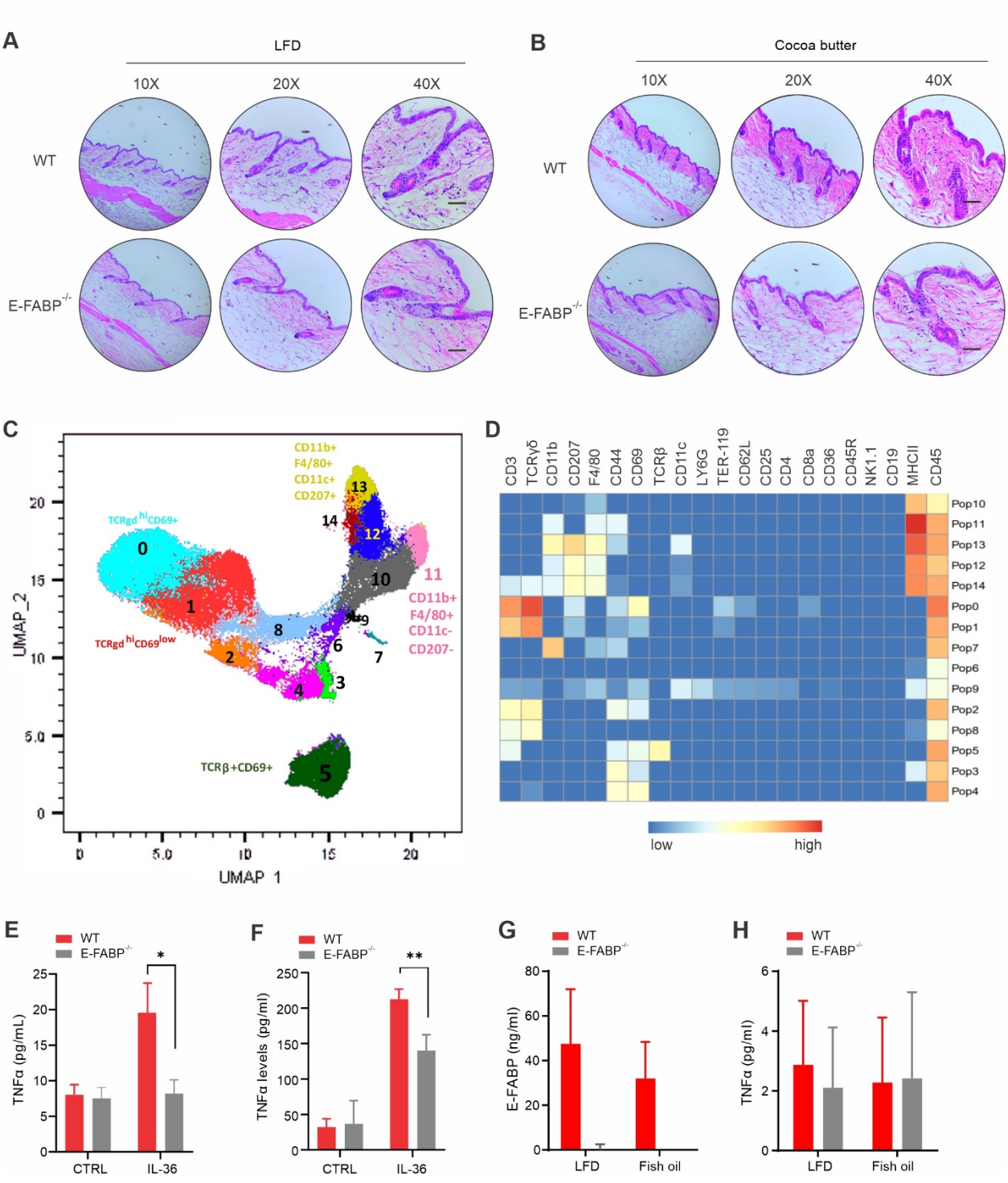

Figure S7. E-FABP deficiency compromises IL-36-induced inflammatory TNFα responses. Related to Figure 7. (A, B) Hematoxylin & eosin staining of skin tissues from WT and E-FABP$^{-/-}$ mice fed the LFD (A), or cocoa butter HFD (B), respectively, for 3 months. Scale bar, 100μM. (C, D) CyTOF-based analysis of skin immune cell signatures in WT and E-FABP$^{-/-}$ mice fed the fish oil HFD for 3 months. Heatmap of individual skin

immune populations is shown in panel D. (E, F) ELISA measurement of supernatants levels of TNFα produced from purified splenic macrophages of WT and E-FABP$^{-/-}$ mice treated with IL-36 (100ng/ml) for 3 hours (E) or 3 days (F). (G, H) ELISA measurement of E-FABP (G) and TNFα (H) in the serum of WT and E-FABP$^{-/-}$ mice fed LFD or fish oil HFD for 3 months (n=7/group). Data are shown as mean ± SD (** $p<0.01$, * $p<0.05$, unpaired Student t test).